remote sensing

MDPI

Communication

Neighbourhood Species Richness Reduces Crown Asymmetry of Subtropical Trees in Sloping Terrain

Maria D. Perles-Garcia [1,2,*], Matthias Kunz [3], Andreas Fichtner [4], Nora Meyer [3], Werner Härdtle [4] and Goddert von Oheimb [3]

1 German Centre for Integrative Biodiversity Research (iDiv), 04103 Leipzig, Germany
2 Institute of Biology/Geobotany and Botanical Garden, Martin Luther University Halle-Wittenberg, 06108 Halle (Saale), Germany
3 Institute of General Ecology and Environmental Protection, Technische Universität Dresden, 01737 Tharandt, Germany; matthias.kunz@tu-dresden.de (M.K.); nora.meyer@tu-dresden.de (N.M.); goddert_v_oheimb@tu-dresden.de (G.v.O.)
4 Institute of Ecology, Leuphana University of Lüneburg, 21335 Lüneburg, Germany; fichtner@leuphana.de (A.F.); werner.haerdtle@leuphana.de (W.H.)
* Correspondence: maria_dolores.perles@idiv.de

Abstract: Reforestation in sloping terrain is an important measure for soil erosion control and sustainable watershed management. The mechanical stability of such reforested stands, however, can be low due to a strong asymmetric shape of tree crowns. We investigated how neighbourhood tree species richness, neighbourhood pressure, tree height, and slope inclination affect crown asymmetry in a large-scale plantation biodiversity-ecosystem functioning experiment in subtropical China (BEF-China) over eight years. We took the advantage of terrestrial laser scanning (TLS) measurements, which provide non-destructive, high-resolution data of tree structure without altering tree interactions. Neighbourhood species richness significantly reduced crown asymmetry, and this effect became stronger at steeper slopes. Our results suggest that tree diversity promotes the mechanical stability of forest stands in sloping terrain and highlight the importance of TLS-data for a comprehensive understanding of the role of tree diversity in modulating crown interactions in mixed-species forest plantations.

Keywords: BEF-China; biodiversity-ecosystem functioning; crown asymmetry; crown complementarity; forestry; LiDAR; sloping terrain; terrestrial laser scanning

Citation: Perles-Garcia, M.D.; Kunz, M.; Fichtner, A.; Meyer, N.; Härdtle, W.; von Oheimb, G. Neighbourhood Species Richness Reduces Crown Asymmetry of Subtropical Trees in Sloping Terrain. *Remote Sens.* **2022**, *14*, 1441. https://doi.org/10.3390/rs14061441

Academic Editors: Guangsheng Chen, Jia Yang and Zoltan Szantoi

Received: 22 February 2022
Accepted: 14 March 2022
Published: 16 March 2022

1. Introduction

Global forest restoration is an essential measure to counteract ongoing biodiversity loss across biomes, and thereby, promoting ecological resilience and securing multiple benefits for people [1,2]. Similarly, (re-)establishing forests on formerly degraded land is a further important measure to halt ongoing global forest loss [3]. Specifically, planting trees at sloping sites, where land-use conflicts are low, has multiple ecological and socio-economic benefits, such as soil resource (e.g., reduction of erosion), watershed protection, or forest food and wood-based energy provisioning [4–7]. Yet, in such areas, restoration, reforestation, and afforestation success largely depends on the mechanical stability of planted trees. Although there is ample evidence why mixed-species forests should be prioritised over monocultures in forest projects [8], the role of (local) tree diversity in modulating the mechanical stability of planted trees in sloping terrain remains largely unknown.

Changes in local biotic and abiotic conditions are often reflected in tree morphological adjustments. There is ample evidence that crown asymmetry is strongly related to competitive neighbourhood interactions [9], as trees try to avoid competitive pressure by adjusting their crown size and architecture relative to neighbour size. Such plastic

responses to environmental conditions are species-specific and can be considered as one aspect of crown plasticity [10–13]. In general, crown plasticity enables trees to improve their light interception by resorting to spaces where light intensity is higher [14]. Given that competition for light is size-asymmetric [15], taller neighbours induce a higher competitive pressure on smaller individuals, which in turn results in a higher crown asymmetry of the suppressed tree [16,17]. Alternatively, crown asymmetry of tall individuals can result from a low competitive neighbourhood pressure when surrounding light conditions are highly heterogeneous and tall, competitive individuals expand their crows in adjacent canopy gaps to improve their light interception [18]. Moreover, it has been shown that light-demanding tree species exhibit a higher plastic response compared to shade-tolerant species, and that, within a given level of shade tolerance, the strength of a species' response to slope inclination depends on its phenotypic plasticity (e.g., broad-leaved vs. coniferous tree species) [19–21]. Neighbour identity is a further potential factor that alters trees' crown shape. For example, light interception was found to be higher in species-mixtures than monocultures [22], most likely due to changes in biomass allocation pattern and branching modes, which in turn result in a higher crown complementarity [13,23–25]. Crown asymmetry can also result from harsh environmental conditions, such as exposure to strong winds [26] or slope inclination. As trees grow larger, they develop larger crowns. Large-sized crowns of trees growing on steep slopes should, therefore, be more affected by gravitropism compared to those with small-sized crowns, leading to a stronger asymmetric expansion of the crown towards the downhill direction of tall trees [9,27,28]. The magnitude of crown asymmetry, however, may regulate a trees' mechanical stability and thereby determine its susceptibility to abiotic disturbances, such as blowdowns and uprooting, ice, or snow break events. As the frequency and severity of extreme weather events are increasing due to climate change, it is important to understand how environmental factors affect crown asymmetry. Particularly, the importance of tree species richness at the local neighbourhood scale in shaping crown asymmetry is not well understood. This, in turn, has high relevance for sustainable forest management, particularly in sloping terrain. Assuming that species rich neighbourhoods promote positive interactions between tree species and, thus, growth and performance of individual trees, the establishment of highly divers reforestations would significantly improve ecosystem functioning and related services such as timber production, carbon sequestration, or erosion control.

When it comes to quantifying crown asymmetry in mixed-species forests, terrestrial laser scanning (TLS) has proven to play an important role [29]. It is a non-destructive state-of-the-art technology that allows to quantify the three-dimensional structure of a given target tree and its surrounding neighbours without altering tree-tree interactions [30]. The high accuracy of TLS data (i.e., at the level of centimetres) offers detailed, high-resolution measures in forests that are difficult to derive from traditional survey methods [31,32] or from other remote sensing technics, such as airborne or mobile/personal laser scanning [33,34]. However, this technique is still expensive and requires personnel trained in the specific software to process the point clouds, so not many long-term studies of crown interactions are available [32]. Here, we used data from a large-scale plantation biodiversity-ecosystem functioning (BEF) experiment (BEF-China; www.bef-china.com, accessed on 21 February 2022), which was performed in subtropical China and planted in 2009 and 2010. Plot species richness ranged from monocultures up to 24 species mixtures [31]. Trees were planted in a regular grid, resulting in an initial maximum of eight neighbours. In total, we evaluated TLS data of 878 trees collected over a period of 8 years to address the follow questions: (i) What are the effects of local neighbourhood conditions (i.e., neighbourhood species richness and neighbourhood pressure) on crown development and crown displacement (CD) of a target tree (considering CD as a measure of crown asymmetry)? (ii) What are the effects of site microtopography (i.e., slope inclination at the spatial scale of an individual tree) on CD of a target tree? (iii) What are the underlying mechanisms of species richness–CD relationships and the modifying impacts of abiotic site conditions? We hypothesised (i) that neighbourhood species richness reduces CD due to

complementarity effects and (ii) that the strength of neighbourhood species richness and neighbourhood pressure effects depend on microtopography.

2. Materials and Methods

2.1. Study Site

The study was conducted in subtropical China at the biodiversity–ecosystem functioning experiment China (BEF-China) platform (29.08°–29.11° N, 117.90°–117.93° E, 100–300 m a.s.l., Figure 1) [35]. The trees of the experiment are representative for subtropical mixed evergreen broadleaved forests. The most common soil types are Cambisols and Regosols, with Acrisols along the slopes and Greysols in the valleys [36]. The mean precipitation of the study area is 1821 mm year^{-1} and the mean annual temperature is 16.7 °C (averaged from 1971 to 2000; [37]. The slope inclination of the terrain ranges between 1° and 53° (2% to 133%) [36]. The BEF-China experiment covers an area of ca. 37 ha. It consists of 566 study plots established in two sites: site A, planted in 2009, and site B, planted in 2010. In each plot, 400 trees were planted following a regular grid of 20 × 20 trees with a distance between them of 1.29 m, so each tree counts with eight direct neighbours. The high tree diversity gradient of BEF China allows us to study the response of the same species in a direct neighbourhood species richness (NSR) ranging from zero (monoculture, all the trees are the same species as the target tree) to six.

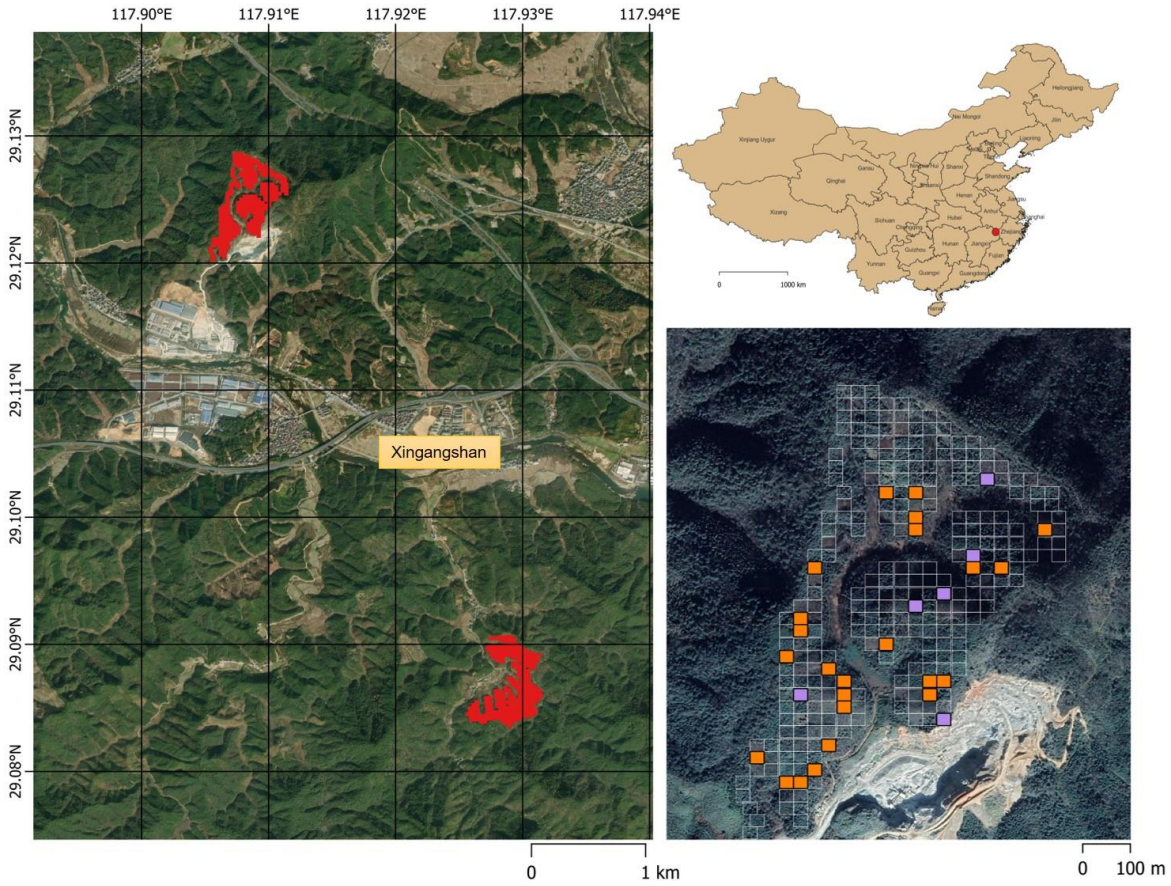

Figure 1. Location of the study site. The top right panel represents the provincial boundary of China, adapted from the Standford Geowebservice WFS (Hijmans, 2015). The location of the study area is represented with a red circle; the left panel shows the location of sites A and B (red polygons) and the closest village (Xingangshan), with the coordinates on the ESRI ArcGIS World Imagery WMS. The bottom right panel shows the studied plots on the ESRI ArcGIS World Imagery WMS: in orange monocultures and two-species mixtures, where nine scan positions were distributed following a regular grid, and in purple the four- and eight-species mixtures, where 16 scan positions were regularly distributed in the centre of the plot.

For this study, we used data from 878 individual trees (i.e., target trees) of the eight tree species *Castanea henryi* (Skan) Rehder & E.H. Wilson, *Castanopsis sclerophylla* (Lindley & Paxton) Schottky, *Choerospondias axillaris* (Roxburgh) B. L. Burtt & A. W. Hill, *Liquidambar formosana* Hance, *Nyssa sinensis* Oliver, *Quercus serrata* Murray, *Sapindus saponaria* Linnaeus, and *Triadica sebifera* (Linnaeus) Small. These target trees grew in 30 study plots from Site A that varied in tree species richness ranging from monoculture to mixtures of 2, 4, and 8 species. All trees were randomly assigned to planting positions before planting, and were planted in a regular grid with a distance of 1.29 m. Further plot information is provided in Table S1.

2.2. Terrestrial Laser Scanning Data

TLS data have been collected during February–March of the years 2012, 2013, 2014, 2015, 2016, and 2019. For the whole period of time, this resulted in a total sample size of 4004 target trees. Table S2 shows an overview of the number and size of the files. Scanning was mainly done using the laser scanner FARO Focus S120, but also the FARO Focus X130 in 2019, and the FARO Photon Scanner in 2013 and 2012 (FARO Europe, Korntal-Münchingen, Germany). The technical specifications of the scanners can be found in Table S3.

The scan positions within the plot were equally distributed, recording the 6 × 6 central trees with 9 scan positions for the monocultures and two-species mixture plots, and the 12 × 12 central trees with 16 scan positions for the four- and eight-species mixture plots (Figure 2) [38]. Ten polystyrene spheres and three quadratic checkerboards were distributed in each plot and used as reflectance targets to co-register the point clouds. We used a spatial resolution equivalent of around 6 mm at a distance of 10 m. The FARO scanner was set up on a levelled tripod around 1.3 m in height. All scans were performed in almost windless conditions.

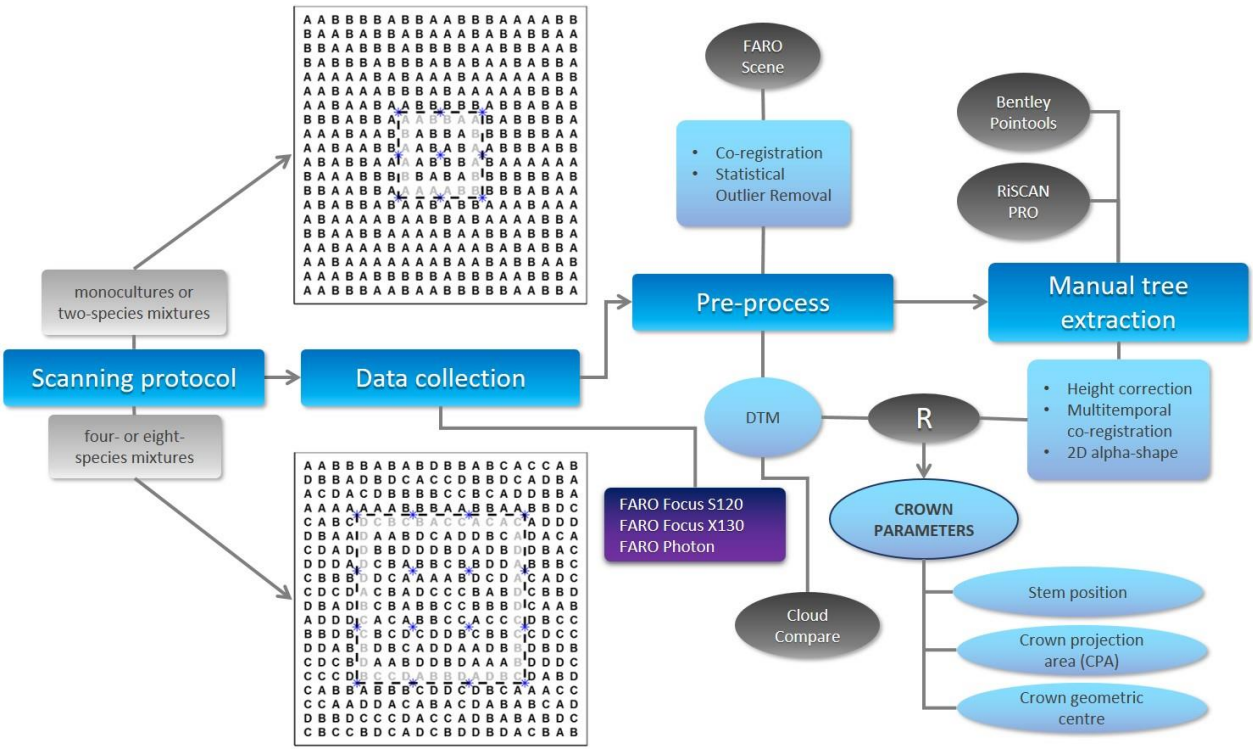

Figure 2. Workflow of data preparation. Schematic representation of the scanning protocol is adapted from Kunz et al. (2019, Figure S1) [13]. There, blue asterisks represent scanning positions, and letters indicate different tree species. Black circles show the used software, while the outcomes are in light blue circles. Main processes are in blue squares and the instruments used are in a purple square.

2.3. TLS Data Processing and Calculation of Crown Displacement

The calculation of CD was based on TLS measurements. To process the TLS data, we used FARO Scene software (V. 5.2.6) to co-register the point clouds of each plot. For the co-registration, mean reference tension did not exceed 0.005. Then, we used a statistical outlier removal to delete stray points and stored each point cloud in a local Cartesian coordinates system (3D coordinates: X, Y, Z). Individual trees were extracted manually using RiSCAN PRO (v2.6.2) and Bentley Pointools (v1.5 Pro). Each tree point cloud was identified by its relative position within the plot and related to the reference targets, and it was stored separately in an ASCII format.

Each of the registered point clouds of the plots in a given year exists in an arbitrary local coordinate system. This is explained by the missing GNSS capabilities of the FARO scanners. In order to compare the trees and the crowns over time, a multi-temporal co-registration into a common reference frame (here UTM Zone 50N, WGS84; EPSG:32650) was required. This was achieved in a two-step approach. First, the tree point clouds of the individual plots were registered relative to each other. The tree positions were registered using a 2D conformal transformation with constant scale in a least squares fashion [39]. The tree positions from the year 2015 were used as references. The scanners, which have an in-built Inertial Measurement Unit (IMU), and the respective point clouds were levelled and rotated with respect to the horizontal level. In order to align the trees to the same height level, we projected the tree positions onto the respective digital terrain model (DTM) and calculated a mean height level for each plot and year. DTMs were extracted using the rasterise tool with the minimum Z coordinate at each grid cell of 5 cm. To avoid below ground points, each DTM was visually inspected before further processing. Possible gaps in the DTM were closed using the raster package in R. A height correction was then applied to the point clouds to achieve a match. In a second step, the local coordinates were transformed in the global coordinate system in the same fashion using the theoretically planned tree locations from the BEF-China data portal (https://data.botanik.uni-halle.de/bef-china/, accessed on 21 February 2022). All multi-temporal co-registrations of the tree positions showed a mean error around zero with normally distributed residuals (SD was between 1 and 3 cm).

For each target tree, we first determined crown projection area (CPA) from a 2D alpha shape [40] of the orthogonal projection of all tree points in the x–y plane. We also computed the geometric centre (centroid point) of the CPA. This point allows us to quantify the overall horizontal direction and magnitude of CD with respect to the planting position of the tree. Two-dimensional alpha shapes were computed in R 3.6.0 using the package [41]. The alpha-value was set to 0.5. The centroid, area, and perimeter of the enclosing polygon were computed using the sp package [42]. The stem position was computed by fitting a circle (least squares procedure) into a horizontal slice (3 cm slice thickness) of the tree point cloud at 5 cm above the ground. CD was calculated as the distance from the vector that goes from the stem position to the centre of the CPA based on the 2D polygon of the CPA (Figure 3a). The complete workflow is represented in Figure 2.

2.4. Explanatory Variables

To identify potential drivers of CD, we used microtopography, target tree height, neighbourhood pressure, and neighbourhood tree species richness as potential explanatory variables.

Microtopography (MT) was calculated as the distance from the stem position to the horizontal unit (one meter) in the direction of the steepest slope [11] (Figure 3b). For each plot and year, data on MT were obtained from the DTM (5 cm grid). Slope and aspect were computed for each tree with bilinear interpolation from the DTM at the respective tree location in the global coordinate system using the terrain function from the raster package in R [43]. The height of each target tree (TH) was calculated as the difference between the highest and lowest z-coordinate of the tree point cloud.

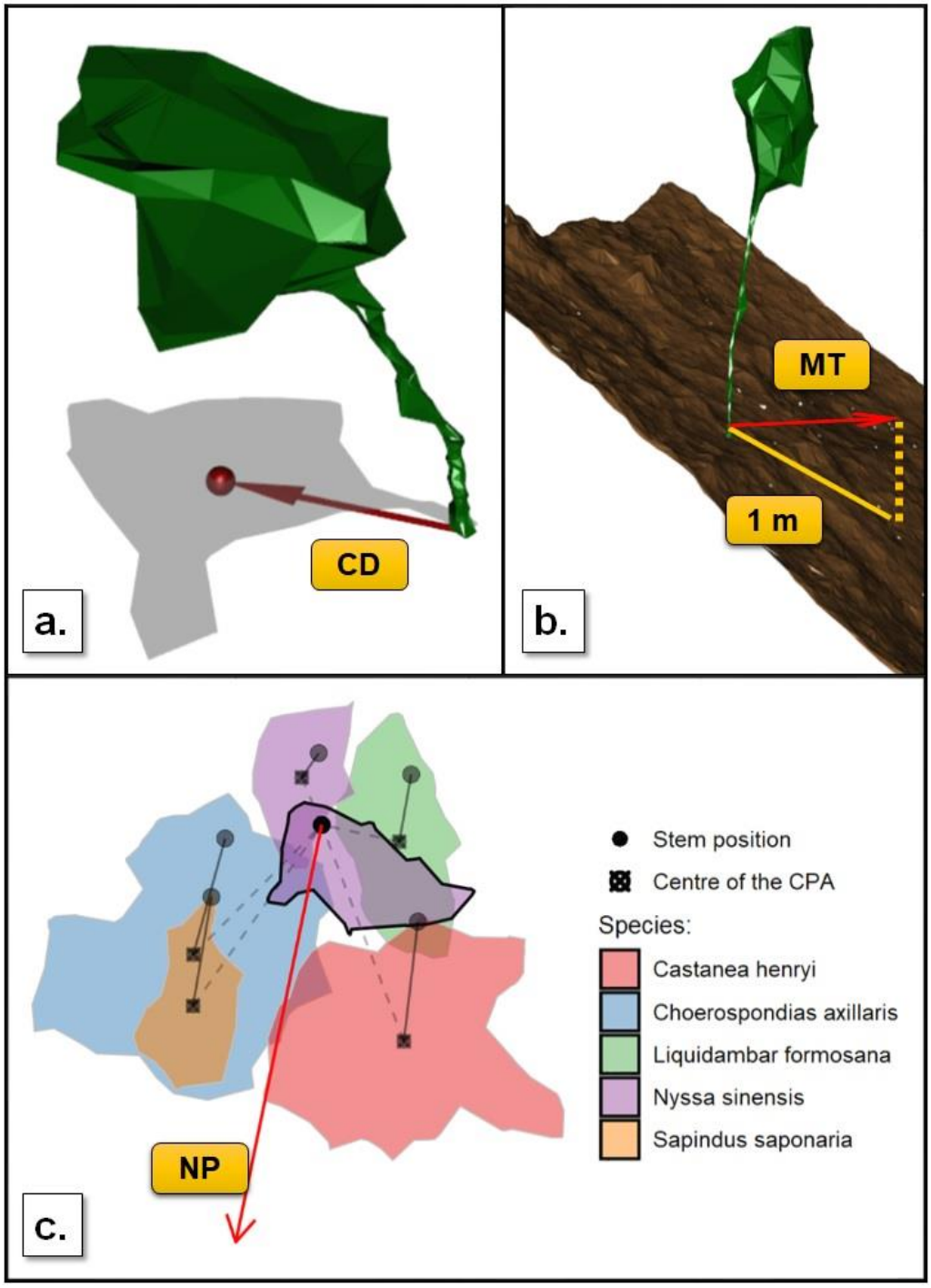

Figure 3. Graphic representation of (**a**) crown displacement, where the crown projection area is shown in grey, the centre is represented as a red dot, and the crown displacement is represented as a red arrow. In green is the alpha shape representation of an individual tree; (**b**) microtopography, showing in brown the terrain, in green the representation of an individual tree, and in red the vector of microtopography; and (**c**) neighbourhood pressure, showing the crown projection area of the target tree (with a black outline) and its direct neighbours. Dots represent the stem position, dots with a cross represent the centre of the crown projection area, solid lines represent the displacement of each neighbour, and dotted lines the pressure from the neighbour to the target tree. The red arrow represents the total neighbourhood pressure. Different polygon colours indicate different tree species.

For each target tree, we calculated an index of neighbourhood pressure (NP, Equation (1)). Other studies assume a linear relation between the size of the tree and its pressure on the

target tree [11,12,26,30,44]. In this study, we, therefore, developed a new parameter that scale the pressure depending on the relative canopy position in respect of the target tree: the canopy level index (c_{li}, Sup. Equation (1)). To account for the crown size of the neighbour and the direction of growth, we also include the CD of the neighbour.

$$NP = \sum_{n} \frac{(CD_n + CP) \times C_{li}}{CP2} \quad (1)$$

NP was calculated using vectors: for each neighbour (n), we sum its vector of CD (CD_n, represented as a solid line in Figure 3c) to the competitive pressure (CP, represented as dotted line in Figure 3c). The resultant vector is escalated by the c_{li} (Sup. Equation (1)), and the result is divided by the squared of the CP. NP is the length of the vector that results from the sum of the individual NP from all direct neighbours (represented as a solid red arrow in Figure 3c).

Neighbourhood tree species richness (NSR) was defined as the number of neighbours that differed in the species identity from the target tree. In this study, this resulted in a gradient of varying levels of NSR ranging from 0 (conspecific neighbours) to 6 (maximum of heterospecific neighbours). To ensure representative NSR-levels, respectively, we excluded those target trees (n = 32; 0.9% of the data) that were surrounded by six heterospecific neighbours (NSR = 6). Consequently, our NSR gradient ranged between zero and five.

2.5. Statistical Analyses

We applied linear mixed-effects models to test the effects of MT, tree size (TH), and neighbourhood conditions (NP and NSR) on CD. We also included the two-way interactions MT * NSR and NP * NSR in the initial model to test for potential NSR dependencies on the CD-MT and the CD-NP relationships. Given the positive relationship between TH and study year (t: 34.97, $p < 0.001$; Figure S3), TH also accounts for the temporal development of the target trees. Species identity of the target tree, neighbourhood tree species composition, and target tree nested in the study plot were used as crossed random effects. Moreover, we included target tree height as a random slope in the model structure, to test for the effect of tree ontogeny (i.e., tree height) depending on species. Including a random slope effect significantly improved the fit of the initial model (ΔAIC: 202.2; $p < 0.001$).

Model selection (backward-approach) was based on likelihood ratio tests with maximum likelihood estimations [45]. The best-fitting model was based on restricted maximum likelihood estimation. CD and VP were square root-transformed prior to analyses to meet model assumptions, which were confirmed by the residual plots of the best-fitting model (Figure S4). Prior to analysis, all predictors were standardised (mean = 0, SD = 1). All analyses were conducted using R (version 4.0.2) and the packages circular, lm4, lmerTest, MuMIn, and sjPlot.

3. Results

The best-fitting model included microtopography (MT), target tree height (TH), neighbourhood pressure (NP), and neighbourhood tree species richness (NSR), as well as the interaction between MT and NSR, and explained 60% (fixed-effects only, marginal R^2) and 85% (fixed and random effects, conditional R^2) of the variation in CD (Table 1). As expected, TH was the strongest predictor for square root-transformed CD, followed by NP (Figure 4; Table 1). Here, CD increased as trees grew larger or experienced a higher NP intensity (Figure 4). Moreover, the positive effect of MT on CD was modulated by NSR (two-way interaction MT * NSR: $\chi^2 = 0.40$, $p = 0.036$; Table 1). CD decreased continuously with increasing NSR, and this effect became stronger with increasing MT (Figure 5a). As a result, CD of trees growing in heterospecific neighbourhoods were 4 % (NSR: 1) to 18% (NSR: 5) lower than in conspecific neighbourhoods on average (Figure 5b). A maximum reduction of CD (33%) was observed for trees on steep slopes (i.e., 51° in our study) growing in species-rich neighbourhoods (NSR: 5; Figure 5b). In contrast, we did not find an NSR dependency of NP effects (two-way interaction NP * NSR: $\chi^2 = 0.32$, $p = 0.571$).

Table 1. Results of mixed-effects model of microtopography (MT), target tree height (TH), neighbourhood pressure (NP, square root-transformed), neighbourhood tree species richness (NSR), and the interaction between MT and NSR on crown displacement (square root-transformed). Parameter estimates are standardised and represent the effect size of the covariates in the model. n = 4004.

	Estimate	SE	df	F	p
MT	0.0109	0.0058	383.3233	3.5242	0.0609
TH	0.2119	0.0187	6.6612	127.8893	<0.001
NP	0.0578	0.0031	3909.9625	355.8978	<0.001
NSR	−0.0244	0.0090	160.9722	7.3146	0.0076
MT * NSR	−0.0111	0.0053	1125.5189	4.3397	0.0375
Marginal R^2		0.60			
Conditional R^2		0.85			
Random effects					
SD (tree tag nested plot)				0.1022	
SD (plot)				0.0601	
SD (species identity)				0.0589	
SD (neighbourhood composition)				0.0511	
SD (tree height)				0.0516	

SE: standard error; df: degrees of freedom; SD: standard deviation.

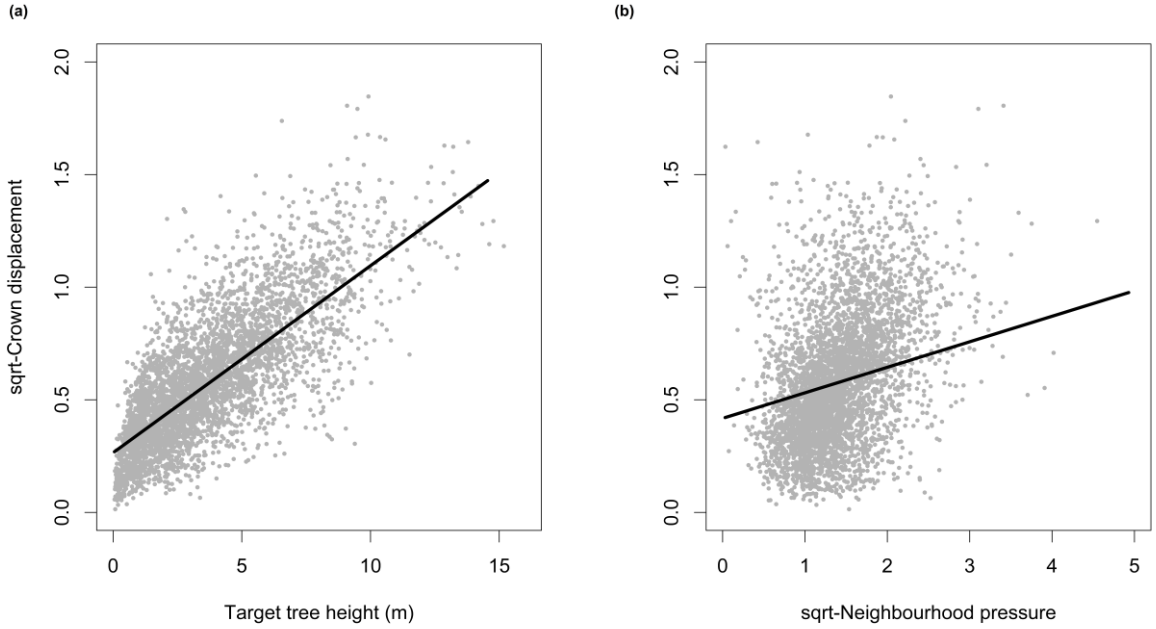

Figure 4. Differences in the strength of the effects of (**a**) target tree height and (**b**) neighbourhood pressure (square root-transformed) on crown displacement (square root-transformed). Lines represent mixed-effects model fits with microtopography and neighbourhood tree species richness kept at their means. Grey points represent observed values.

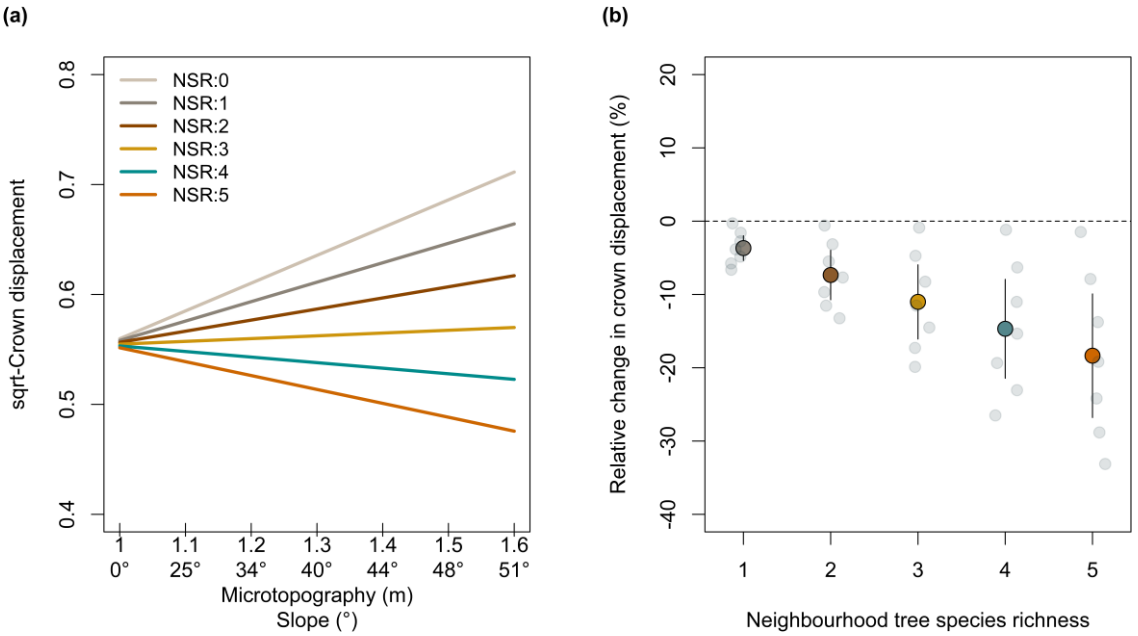

Figure 5. (**a**) Effects of microtopography (MT) on crown displacement (square root-transformed) with varying levels of neighbourhood tree species richness (NSR). Lines represent mixed-effects model fits (with target tree height and neighbourhood pressure kept at its mean). X-axis shows MT in meters and its conversion to slope in degrees. (**b**) Relative changes (%) in crown displacement between conspecific neighbourhoods (NSR: 0) and heterospecific neighbourhoods (NSR: 1–5). Dots represent predicted means based on a mixed-effects model (with target tree height kept at its mean), and error bars indicate the 95% confidence interval of the prediction. Grey points (slightly jittered to facilitate visibility) represent predictions for each level of the microtopography gradient ranging from 1 to 1.6 (see panel (**a**)).

4. Discussion

Based on an eight-year TLS measurement series on tree growth in the BEF-China experiment, our study provides evidence that NSR has the potential to significantly reduce the CD of trees growing in sloping terrain. We hypothesise that this finding is mainly attributable to the effects of interspecific niche complementarity between neighbouring trees, which increases with increasing tree NSR [46]. There is evidence that increasing NSR increases the probability of neighbouring trees to differ with regard to growth-related functional traits, which in turn affect tree–tree interactions in diverse neighbourhoods. For example, functional richness-related differences in crown traits, biomass allocation patterns, or light requirements are important drivers of crown complementarity and may, therefore, reduce interspecific competition between neighbouring trees [21,24,25,47,48]. As a result, NSR may improve tree crown complementarity (also in a physical sense) and, thus, decreases CD as an expression of decreasing competitive interactions. This interpretation is in agreement with previous studies which have shown that tree species differ in biomass allocation patterns when comparing their growth behaviour in mixtures and monocultures (increasing crown plasticity in mixtures; [23,24]). Thus, high functional diversity (with regard to growth-related traits) allows tree canopies to complement each other without increasing asymmetry. This is particularly important in the context of forests growing on slopes, as it could potentially increase individual tree survival by reducing the risk of stem breakage, and thus, enhance stand stability.

Interestingly, we also found a significant interaction effect between MT and NSR, which negatively affects CD (partly confirming our second hypothesis). As indicated by Figure 5a, CD decreases with decreasing MT for conspecific neighbourhoods, but increases with decreasing MT for heterospecific neighbourhoods. These findings suggest that intraspecific competition (i.e., in conspecific neighbourhoods and monocultures, respectively)

increases with increasing MT, which in turn forces trees to a higher crown displacement, e.g., for minimising overshading (i.e., competition for light [16,19]). In contrast, trees in heterospecific neighbourhoods benefit from a diverse neighbourhood with increasing MT, since complementarity effects (e.g., attributable to different light requirements of different tree species) may minimise neighbourhood pressure and, thus, CD [21,49]. In this context, it is important to note that the CD of trees could also increase with increasing MT due to physical displacement mechanisms, e.g., because trees might tend to overturn downslope due to unstable substrate conditions. However, this process is effective across tree species and different neighbourhood richness levels and, thus, cannot explain the negative NSR and MT * NSR effects on CD. However, our findings did not support our expectation that NSR effects on CD are mediated by NP (i.e., we found no significant NP×NSR interaction). This suggests that NP is strongly co-determined by tree height, which in turn affects CD (see below) and is effective regardless of NSR.

TH proved to be the strongest predictor of CD, with a positive relationship between CD and TH. This contradicts findings from tropical forests, according to which TH and CD were negatively correlated [16]. Our results suggest that trees growing on sloping terrain develop asymmetric crowns already at an early stage, and this asymmetry becomes stronger over time, that is, with proceeding growth of the trees. It is likely that differences in TH are a driver of overshading, particularly for trees growing downslope, which forces them to develop asymmetric crowns to improve light access. High CD, in turn, could be problematic for the survival of trees in the longer term, because a strongly asymmetric crown growing on a steep slope could challenge the trees' capability to physically stabilise its crown architecture against gravity forces [10], but also increases the risk of stem breakage.

In addition to TH, NP also proved to be an important predictor for CD, since NP strengthened CD (according to the model prediction) and was closely positively correlated with CD (r = 0.73, Figure S2). This is consistent with previous studies, which also showed a strong impact of NP on CD [11,12,50,51]. Some studies found no significant effect of NP on CD, but showed a close correlation between the direction of NP and CD [30,44]. A main mechanism underlying our findings could be that competitive interactions increase with increasing NP (e.g., for resources such as light). Increasing CD, thus, indicates that trees attempt to avoid overshading (e.g., by upslope individuals), and therefore, re-position their crowns. This is accompanied by a trade-off between morphological plasticity and mechanical stability, and thus, high CD may decrease the mechanical stability of trees and forest stands. CD, therefore, could be considered as an adaptive mechanism to avoid competition for solar radiation by searching for canopy gaps. Since our refined equation for capturing neighbourhood pressure effects (Sup. methods) significantly improved the fit of the initial model (ΔAIC: 135, $p < 0.001$; Table S2) compared to the index proposed by Brisson and Reynolds [52], it is likely that the relative position of the neighbour crown and its asymmetry constitute an important driver for crown asymmetry.

MT proved to be a third significant driver of CD. Even though several studies already showed that MT had a positive effect on CD [9,11,53–55], we can substantiate this based on data from a controlled experimental setting. MT strongly impacts CD, because trees tend to grow downslope to avoid overshading and to improve light availability [55]. This interpretation is supported by our finding that the direction of the CD was highly positively correlated with the direction of MT (Figure S2) Importantly, this downhill orientation of the tree crowns emerged rapidly, since it was already developed within the first study years (i.e., only a few years after planting). The consequences of our findings for sustainable forest management are discussed in the following conclusion section (see also [56–58]).

5. Conclusions

Reforestation of sloping terrain is an important measure to counteract the adverse effects of former clear-cuts and to improve ecosystem services related to the reestablishment of forest ecosystems. Forest restoration, particularly in sloping areas, improves carbon sequestration, stabilises slopes by preventing soil erosion, improves groundwater recharge,

and may improve timber supply for local people. However, many forest restoration projects, particularly in the tropics and subtropics, made use of few or even only one tree species, despite a broad spectrum of native tree species typical of natural forests of these regions. Thus, resulting monocultures often show limited functions, for example in terms of productivity or stability with regard to extreme weather events, but also miss the opportunity to support high biodiversity, which in turn stabilises food webs and contributes to improved ecosystem functioning.

The present study provides further evidence for the use of a diverse spectrum of tree species in the context of reforestation projects and sustainable forest management practices, particularly for sloping terrain. Our results suggest that tree species richness at the local neighbourhood scale also plays a crucial role for the patterns of tree crown development at sloping sites, as neighbourhood tree species richness minimises crown displacement, most likely as a result of complementarity effects increasing with an increasing neighbourhood species richness. This in turn indicates that tree diversity has the potential to physically stabilise tree growth at sloping sites, reduces the risk of stem breakage or blowdowns, and improves the quality of timber due to the formation of stems with lower CD. As a consequence, sustainable forest management should therefore use the widest possible range of tree species that are natural and representative for a given area. In this way, forestry could improve the functioning of forest plantations (e.g., in the context of reforestation projects) and related ecosystem services such as timber production, carbon sequestration, or erosion control. In summary, our findings stress the importance of tree diversity for forest stability and may encourage forest restoration projects to use a high number of native tree species, particularly in the face of ongoing global environmental shifts such as climate change.

Supplementary Materials: The following supporting information can be downloaded at: https://www.mdpi.com/article/10.3390/rs14061441/s1, Supporting Methods: Neighbourhood pressure (NP); Table S1: Included plots and their characteristics; Table S2: Overview of mean file size (and standard deviation) in Mb for each year and plot. In addition, the number of scans is given for each plot; Table S3: Technical specification of the three FARO scanners based on the technical fact sheets by FARO (Korntal-Münchingen, Germany); Table S4: Model comparison using different calculations of neighbourhood pressure index; Figure S1: Representation of possible inaccuracies when using (a) crown projection area or (b) height as size measurement for the neighbourhood pressure index; Figure S2: Curve of the function for the canopy level index (cli); Figure S3: Correlations between the direction of crown displacement (CD), microtopography (MT), and neighbourhood pressure (NP); Figure S4: Boxplot showing the relationship between tree height and study year; Figure S5: Residual plots of the best-fitting model.

Author Contributions: Conceptualisation, M.D.P.-G., G.v.O., W.H. and M.K.; methodology, M.D.P.-G., N.M. and M.K.; software, M.D.P.-G., N.M., A.F. and M.K.; validation, A.F.; formal analysis, M.D.P.-G., M.K. and A.F.; investigation, M.D.P.-G. and M.K.; resources, G.v.O. and W.H.; data curation, M.D.P.-G., M.K. and A.F.; writing—original draft preparation, M.D.P.-G.; writing—review and editing, M.D.P.-G., G.v.O., A.F., W.H., M.K. and N.M.; visualisation, M.D.P.-G. and A.F.; supervision, G.v.O.; project administration, G.v.O. and W.H.; funding acquisition, G.v.O. and W.H. All authors have read and agreed to the published version of the manuscript.

Funding: This research was funded by the Deutsche Forschungsgemeinschaft (DFG, German Research Foundation), grant number 319936945/GRK2324, and by the University of Chinese Academy of Sciences (UCAS).

Institutional Review Board Statement: Not applicable.

Informed Consent Statement: Not applicable.

Data Availability Statement: Data available under request via the BEF-China project database: https://data.botanik.uni-halle.de/bef-china/datasets/654, accessed on 21 February 2022 (Perles-Garcia et al., 2022).

Acknowledgments: We are grateful to the local workers and to M. Hildebrand and G. Hähn, who assisted to conduct the scans in the field, to A. Koller and I. Frehse, who contributed processing the data, to R. Vidaurre and A. Vovides, who supported the development of the methodology, and to the BEF-China coordination team for continuous logistical support.

Conflicts of Interest: The authors declare no conflict of interest. The funders had no role in the design of the study; in the collection, analyses, or interpretation of data; in the writing of the manuscript, or in the decision to publish the results.

References

1. Brancalion, P.H.S.; Niamir, A.; Broadbent, E.; Crouzeilles, R.; Barros, F.S.M.; Almeyda Zambrano, A.M.; Baccini, A.; Aronson, J.; Goetz, S.; Leighton Reid, J.; et al. Global restoration opportunities in tropical rainforest landscapes. *Sci. Adv.* **2019**, *5*, 1–12. [CrossRef] [PubMed]
2. Fichtner, A.; Härdtle, W. Forest Ecosystems: A Functional and Biodiversity Perspective. In *Perspectives for Biodiversity and Ecosystems*; Hobohm, C., Ed.; Springer International Publishing: Cham, Switzerland, 2021; pp. 383–405, ISBN 978-3-030-57710-0.
3. FAO. *Global Forest Resources Assessment 2020: Main Report*; FAO: Rome, Italy, 2020.
4. Lamb, D.; Erskine, P.D.; Parrotta, J.A. Restoration of degraded tropical forest landscapes. *Science* **2005**, *310*, 1628–1632. [CrossRef] [PubMed]
5. Jagger, P.; Pender, J. The role of trees for sustainable management of less-favored lands: The case of eucalyptus in Ethiopia. *For. Policy Econ.* **2003**, *5*, 83–95. [CrossRef]
6. Wenhua, L. Degradation and restoration of forest ecosystems in China. *For. Ecol. Manag.* **2004**, *201*, 33–41. [CrossRef]
7. Hou, G.; Delang, C.O.; Lu, X. Afforestation changes soil organic carbon stocks on sloping land: The role of previous land cover and tree type. *Ecol. Eng.* **2020**, *152*, 105860. [CrossRef]
8. Lewis, S.L.; Wheeler, C.E.; Mitchard, E.T.A.; Koch, A. Restoring natural forests is the best way to remove atmospheric carbon. *Nature* **2019**, *568*, 25–28. [CrossRef]
9. Lang, A.C.; Härdtle, W.; Bruelheide, H.; Geißler, C.; Nadrowski, K.; Schuldt, A.; Yu, M.; von Oheimb, G. Tree morphology responds to neighbourhood competition and slope in species-rich forests of subtropical China. *For. Ecol. Manag.* **2010**, *260*, 1708–1715. [CrossRef]
10. Valladares, F.; Gianoli, E.; Gómez, J.M. Ecological limits to plant phenotypic plasticity. *New Phytol.* **2007**, *176*, 749–763. [CrossRef]
11. Umeki, K. Modeling the relationship between the asymmetry in crown display and local environment. *Ecol. Modell.* **1995**, *82*, 11–20. [CrossRef]
12. Schröter, M.; Härdtle, W.; von Oheimb, G. Crown plasticity and neighborhood interactions of European beech (*Fagus sylvatica* L.) in an old-growth forest. *Eur. J. For. Res.* **2012**, *131*, 787–798. [CrossRef]
13. Kunz, M.; Fichtner, A.; Härdtle, W.; Raumonen, P.; Bruelheide, H.; von Oheimb, G. Neighbour species richness and local structural variability modulate aboveground allocation patterns and crown morphology of individual trees. *Ecol. Lett.* **2019**, *22*, 2130–2140. [CrossRef] [PubMed]
14. Uria-Diez, J.; Pommerening, A. Crown plasticity in Scots pine (*Pinus sylvestris* L.) as a strategy of adaptation to competition and environmental factors. *Ecol. Modell.* **2017**, *356*, 117–126. [CrossRef]
15. Schwinning, S.; Weiner, J. Mechanisms the degree of size asymmetry determining in competition among plants. *Oecologia* **2012**, *113*, 447–455. [CrossRef] [PubMed]
16. Young, T.P.; Hubbell, S.P. Crown asymmetry, treefalls, and repeat disturbance of broad-leaved forest gaps. *Ecology* **1991**, *72*, 1464–1471. [CrossRef]
17. Longuetaud, F.; Piboule, A.; Wernsdörfer, H.; Collet, C. Crown plasticity reduces inter-tree competition in a mixed broadleaved forest. *Eur. J. For. Res.* **2013**, *132*, 621–634. [CrossRef]
18. Muth, C.C.; Bazzaz, F.A. Tree canopy displacement and neighborhood interactions. *Can. J. For. Res.* **2003**, *33*, 1323–1330. [CrossRef]
19. Niinemets, Ü. A review of light interception in plant stands from leaf to canopy in different plant functional types and in species with varying shade tolerance. *Ecol. Res.* **2010**, *25*, 693–714. [CrossRef]
20. Böhnke, M.; Bruelheide, H. How do evergreen and deciduous species respond to shade?—Tolerance and plasticity of subtropical tree and shrub species of South-East China. *Environ. Exp. Bot.* **2013**, *87*, 179–190. [CrossRef]
21. Jucker, T.; Bouriaud, O.; Coomes, D.A. Crown plasticity enables trees to optimize canopy packing in mixed-species forests. *Funct. Ecol.* **2015**, *29*, 1078–1086. [CrossRef]
22. Duarte, M.M.; de Moral, R.A.; Guillemot, J.; Zuim, C.I.F.; Potvin, C.; Bonat, W.H.; Stape, J.L.; Brancalion, P.H.S. High tree diversity enhances light interception in tropical forests. *J. Ecol.* **2021**, *109*, 2597–2611. [CrossRef]
23. Guillemot, J.; Kunz, M.; Schnabel, F.; Fichtner, A.; Madsen, C.P.; Gebauer, T.; Härdtle, W.; von Oheimb, G.; Potvin, C. Neighbourhood-mediated shifts in tree biomass allocation drive overyielding in tropical species mixtures. *New Phytol.* **2020**, *228*, 1256–1268. [CrossRef] [PubMed]

24. Hildebrand, M.; Perles-Garcia, M.D.; Kunz, M.; Härdtle, W.; von Oheimb, G.; Fichtner, A. Tree-tree interactions and crown complementarity: The role of functional diversity and branch traits for canopy packing. *Basic Appl. Ecol.* **2021**, *50*, 217–227. [CrossRef]
25. Williams, L.J.; Paquette, A.; Cavender-Bares, J.; Messier, C.; Reich, P.B. Spatial complementarity in tree crowns explains overyielding in species mixtures. *Methods Ecol. Evol.* **2017**, *1*, 63. [CrossRef] [PubMed]
26. Vovides, A.G.; Berger, U.; Grueters, U.; Guevara, R.; Pommerening, A.; Lara-Domínguez, A.L.; López-Portillo, J. Change in drivers of mangrove crown displacement along a salinity stress gradient. *Funct. Ecol.* **2018**, *32*, 2753–2765. [CrossRef]
27. Umeki, K. Importance of crown position and morphological plasticity in competitive interaction in a population of Xanthium canadense. *Ann. Bot.* **1995**, *75*, 259–265. [CrossRef]
28. Matsuzaki, J.; Masumori, M.; Tange, T. Stem phototropism of trees: A possible significant factor in determining stem inclination on forest slopes. *Ann. Bot.* **2006**, *98*, 573–581. [CrossRef] [PubMed]
29. Calders, K.; Adams, J.; Armston, J.; Bartholomeus, H.; Bauwens, S.; Bentley, L.P.; Chave, J.; Danson, F.M.; Demol, M.; Disney, M.; et al. Terrestrial laser scanning in forest ecology: Expanding the horizon. *Remote Sens. Environ.* **2020**, *251*, 112102. [CrossRef]
30. Seidel, D.; Leuschner, C.; Müller, A.; Krause, B. Crown plasticity in mixed forests-Quantifying asymmetry as a measure of competition using terrestrial laser scanning. *For. Ecol. Manag.* **2011**, *261*, 2123–2132. [CrossRef]
31. Newnham, G.J.; Armston, J.D.; Calders, K.; Disney, M.I.; Lovell, J.L.; Schaaf, C.B.; Strahler, A.H.; Danson, F.M. Terrestrial laser scanning for plot-scale forest measurement. *Curr. For. Rep.* **2015**, *1*, 239–251. [CrossRef]
32. Liang, X.; Kankare, V.; Hyyppä, J.; Wang, Y.; Kukko, A.; Haggrén, H.; Yu, X.; Kaartinen, H.; Jaakkola, A.; Guan, F.; et al. Terrestrial laser scanning in forest inventories. *ISPRS J. Photogramm. Remote Sens.* **2016**, *115*, 63–77. [CrossRef]
33. Bienert, A.; Georgi, L.; Kunz, M.; Maas, H.G.; von Oheimb, G. Comparison and combination of mobile and terrestrial laser scanning for natural forest inventories. *Forests* **2018**, *9*, 395. [CrossRef]
34. Jung, S.E.; Kwak, D.A.; Park, T.; Lee, W.K.; Yoo, S. Estimating crown variables of individual trees using airborne and terrestrial laser scanners. *Remote Sens.* **2011**, *3*, 2346–2363. [CrossRef]
35. Bruelheide, H.; Nadrowski, K.; Assmann, T.; Bauhus, J.; Both, S.; Buscot, F.; Chen, X.Y.; Ding, B.; Durka, W.; Erfmeier, A.; et al. Designing forest biodiversity experiments: General considerations illustrated by a new large experiment in subtropical China. *Methods Ecol. Evol.* **2014**, *5*, 74–89. [CrossRef]
36. Scholten, T.; Goebes, P.; Kuhn, P.; Seitz, S.; Assmann, T.; Bauhus, J. On the combined effect of soil fertility and topography on tree growth in subtropical forest ecosystems'a study from SE China. *J. Plant Ecol.* **2017**, *10*, 111–127. [CrossRef]
37. Yang, X.; Bauhus, J.; Both, S.; Fang, T.; Härdtle, W.; Kröber, W.; Ma, K.; Nadrowski, K.; Pei, K.; Scherer-Lorenzen, M.; et al. Establishment success in a forest biodiversity and ecosystem functioning experiment in subtropical China (BEF-China). *Eur. J. For. Res.* **2013**, *132*, 593–606. [CrossRef]
38. Li, Y.; Hess, C.; von Wehrden, H.; Härdtle, W.; von Oheimb, G. Assessing tree dendrometrics in young regenerating plantations using terrestrial laser scanning. *Ann. For. Sci.* **2014**, *71*, 453–462. [CrossRef]
39. Ghilani, C.D.; Wolf, P.R. *Adjustment Computations: Spatial Data Analysis*, 5th ed.; Wiley: Hoboken, NJ, USA, 2010.
40. Edelsbrunner, H.; Kirkpatrick, D.; Seidel, R. On the shape of a set of points in the plane. *IEEE Trans. Inf. Theory* **1983**, *29*, 551–559. [CrossRef]
41. Pateiro-Lopez, B.; Rodriguez-Casal, A. *alphahull Generalization of the Convex Hull of a Sample of Points in the Plane 2019*; R Project: Vienna, Austria, 2019.
42. Bivand, R.S.; Pebesma, E.; Gomez-Rubio, V. *Applied Spatial Data Analysis with R*, 2nd ed.; Springer: New York, NY, USA, 2013.
43. Hijmans, R.J. *raster: Geographic Data Analysis and Modeling*; R Project: Vienna, Austria, 2020.
44. Brisson, J. Neighborhood competition and crown asymmetry in Acer saccharum. *Can. J. For. Res.* **2001**, *31*, 2151–2159. [CrossRef]
45. Zuur, A.F.; Ieno, E.N.; Walker, N.S.; Smith, G.M. *Mixed Effects Models and Extensions in Ecology with R*; R Project: Vienna, Austria, 2009; ISBN 9780429576966.
46. Niklaus, P.A.; Baruffol, M.; He, J.S.; Ma, K.; Schmid, B. Can niche plasticity promote biodiversity–productivity relationships through increased complementarity? *Ecology* **2017**, *98*, 1104–1116. [CrossRef]
47. Schmid, B.; Niklaus, P.A. Biodiversity: Complementary canopies. *Nat. Ecol. Evol.* **2017**, *1*, 0104. [CrossRef]
48. Ali, A.; Lin, S.L.; He, J.K.; Kong, F.M.; Yu, J.H.; Jiang, H.S. Tree crown complementarity links positive functional diversity and aboveground biomass along large-scale ecological gradients in tropical forests. *Sci. Total Environ.* **2019**, *656*, 45–54. [CrossRef] [PubMed]
49. Fichtner, A.; Härdtle, W.; Bruelheide, H.; Kunz, M.; Li, Y.; von Oheimb, G. Neighbourhood interactions drive overyielding in mixed-species tree communities. *Nat. Commun.* **2018**, *9*, 1144. [CrossRef] [PubMed]
50. Lang, A.C.; von Oheimb, G.; Scherer-Lorenzen, M.; Yang, B.; Trogisch, S.; Bruelheide, H.; Ma, K.; Härdtle, W. Mixed afforestation of young subtropical trees promotes nitrogen acquisition and retention. *J. Appl. Ecol.* **2014**, *51*, 224–233. [CrossRef]
51. Aakala, T.; Shimatani, K.; Abe, T.; Kubota, Y.; Kuuluvainen, T. Crown asymmetry in high latitude forests: Disentangling the directional effects of tree competition and solar radiation. *Oikos* **2016**, *125*, 1035–1043. [CrossRef]
52. Brisson, J.; Reynolds, J.F. The effect of neighbors on root distribution in a creosotebush (Larrea Tridentata) population. *Ecology* **1994**, *75*, 1693–1702. [CrossRef]
53. Ehbrecht, M.A. Quantifying Three-Dimensional Stand Structure and Its Relationship with Forest Management and Microclimate in Temperate Forest Ecosystems. Ph.D. Thesis, Georg-August-Universität Göttingen, Göttingen, Germany, 2018.

54. Getzin, S.; Wiegand, K. Asymmetric tree growth at the stand level: Random crown patterns and the response to slope. *For. Ecol. Manage.* **2007**, *242*, 165–174. [CrossRef]
55. Sumida, A.; Terazawa, I.; Togashi, A.; Komiyama, A. Spatial arrangement of branches in relation to slope and neighbourhood competition. *Ann. Bot.* **2002**, *89*, 301–310. [CrossRef]
56. Song, Z.; Seitz, S.; Li, J.; Goebes, P.; Schmidt, K.; Kühn, P.; Shi, X.; Scholten, T. Tree diversity reduced soil erosion by affecting tree canopy and biological soil crust development in a subtropical forest experiment. *For. Ecol. Manag.* **2019**, *444*, 69–77. [CrossRef]
57. Schuldt, A.; Ebeling, A.; Kunz, M.; Staab, M.; Guimarães-Steinicke, C.; Bachmann, D.; Buchmann, N.; Durka, W.; Fichtner, A.; Fornoff, F.; et al. Multiple plant diversity components drive consumer communities across ecosystems. *Nat. Commun.* **2019**, *10*, 1460. [CrossRef]
58. Fichtner, A.; Härdtle, W.; Li, Y.; Bruelheide, H.; Kunz, M.; von Oheimb, G. From competition to facilitation: How tree species respond to neighbourhood diversity. *Ecol. Lett.* **2017**, *20*, 892–900. [CrossRef]